Bioorganic & Medicinal Chemistry Letters 18 (2008) 4267–4274

Contents lists available at ScienceDirect

Bioorganic & Medicinal Chemistry Letters

journal homepage: www.elsevier.com/locate/bmcl

Structural modifications of *N*-arylamide oxadiazoles: Identification of *N*-arylpiperidine oxadiazoles as potent and selective agonists of CB_2

Erin F. DiMauro [a,*], John L. Buchanan [a], Alan Cheng [b], Renee Emkey [c], Stephen A. Hitchcock [f], Liyue Huang [d], Ming Y. Huang [e], Brett Janosky [d], Josie H. Lee [c], Xingwen Li [e], Matthew W. Martin [a], Susan A. Tomlinson [a], Ryan D. White [a], Xiao Mei Zheng [a], Vinod F. Patel [a], Robert T. Fremeau Jr. [e]

[a] *Department of Medicinal Chemistry, Amgen Inc., One Kendall Square, Building 1000, Cambridge, MA 02139, USA*
[b] *Department of Molecular Structure, Amgen Inc., One Kendall Square, Building 1000, Cambridge, MA 02139, USA*
[c] *Department of HTS and Molecular Pharmacology, Amgen Inc., One Kendall Square, Building 1000, Cambridge, MA 02139, USA*
[d] *Department of Pharmacokinetics & Drug Metabolism, Amgen Inc., One Kendall Square, Building 1000, Cambridge, MA 02139, USA*
[e] *Department of Neuroscience, Amgen Inc., One Amgen Center Drive, Thousand Oaks, CA 91320, USA*
[f] *Department of Medicinal Chemistry, Amgen Inc., One Amgen Center Drive, Thousand Oaks, CA 91320, USA*

ARTICLE INFO

Article history:
Received 27 May 2008
Revised 26 June 2008
Accepted 30 June 2008
Available online 3 July 2008

Keywords:
Cannabinoid G-protein coupled receptors
CB2 agonists
Piperidine oxadiazoles

ABSTRACT

Structural modifications to the central portion of the *N*-arylamide oxadiazole scaffold led to the identification of *N*-arylpiperidine oxadiazoles as conformationally constrained analogs that offered improved stability and comparable potency and selectivity. The simple, modular scaffold allowed for the use of expeditious and divergent synthetic routes, which provided two-directional SAR in parallel. Several potent and selective agonists from this novel ligand class are described.

The cannabinoid G-protein coupled receptors, CB_1 and CB_2, play important roles in the transduction and perception of pain.[1] The contribution of CB_1 to the modulation of antinociception has been well established.[1] However, agonism of CB_1, which is predominantly expressed in the CNS, results in undesirable psychotropic effects, sedation, and catalepsy.[2] Selective agonism of CB_2, which is predominantly expressed in immune cells and tissues, presents an opportunity for pain management without the unfavorable CNS side effects. Indeed, a number of CB_2-selective agonists have shown efficacy in rodent models of inflammatory and neuropathic pain at doses that do not cause sedation or locomotor impairment.[3]

In accordance with our ongoing efforts to identify small molecule agonists of CB_2 for use as therapeutic agents in the treatment of pain, we recently disclosed the *N*-arylamide oxadiazoles.[4] This series is represented by **1** (Scheme 1), which exhibits full agonism[5] of the CB_2 receptor at low nanomolar concentrations with >200-fold selectivity over CB_1 in a functional GTP-Eu binding assay (Table 1).[6] Unfortunately, **1** suffered from high clearance in vivo (rat i.v. CL = 5.7 L/h/kg). High clearance was also observed for several of its analogs, and hydrolysis of the amide bond was identified as a major metabolic pathway in rats (Scheme 1).[7]

In an effort to improve the metabolic stability without compromising the agonist potency and efficacy, we investigated reversed amide **3** and propylamines **4**–**6** (Table 1).[8] The reversed amide **3** proved to be significantly less potent and efficacious than **1**. Next, we explored the removal of the amide carbonyl leading to propylamine **4**,[4] which was only 5-fold less potent and selective than the corresponding amide (**1**). Unfortunately, **4** was metabolically unstable in liver microsomes.[7] Accordingly, α-methyl substituents were introduced to block the potential oxidative metabolism, affording secondary and tertiary propylamines ((±)-**5** and **6**). In the case of the mono-methyl analog (±)-**5** only a modest 7-fold loss of potency was observed. The gem di-methyl analog **6** led to a more significant 20-fold loss of potency and provided only a partial agonist (E_{max} = 52%). Also, both compounds were still rapidly metabolized in liver microsomes.

The data from propylamines **4**–**6** suggested that the carbonyl functionality was not essential for potency and efficacy. Furthermore, the 20- to 100-fold selectivity afforded by **4**–**6** was unanticipated since the vast majority of CB_2-selective functional agonists contain amide or sulfone moieties.[3c–f,9] Encouraged by this discovery, we sought to explore cyclic tethers that could presumably improve the metabolic stability and intrinsic potency through

* Corresponding author. Tel.: +1 617 444 5189; fax: +1 617 621 3907.
E-mail address: edimauro@amgen.com (E.F. DiMauro).

0960-894X/$ - see front matter © 2008 Elsevier Ltd. All rights reserved.
doi:10.1016/j.bmcl.2008.06.096

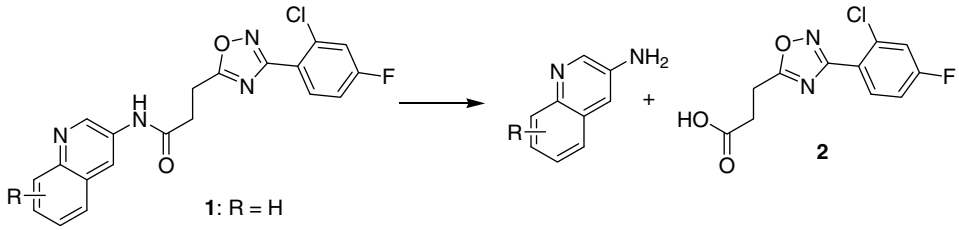

Scheme 1. Amide oxadiazoles and hydrolysis products.

Table 1
Functional GTP-Eu assay results for compounds **1**–**6** (EC_{50}, μM; E_{max}, %) and $CL_{int.}$ in rat and human liver microsomes (RLM, HLM)[a]

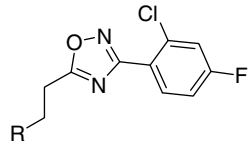

Compound	R	CB_2 EC_{50} (E_{max})	CB_1 EC_{50} (E_{max})	$CL_{int.}$ (μL/min/mg)	
				RLM	HLM
1	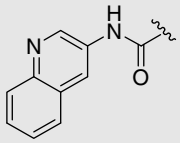	0.002 (115)	0.403 (51)	126	49
2		NA (10)	NA (0.3)	–	–
3	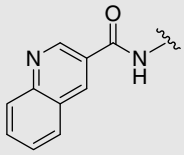	1.55 (87)	NA (−1)	–	–
4	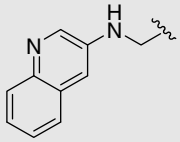	0.011 (104)	0.472 (103)	614	179
(±)-**5**	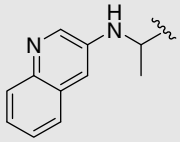	0.015 (112)	1.56 (69)	>399	142
6	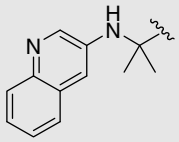	0.053 (52)	1.30 (70)	775	429

[a] The results are expressed as the means SEM for n = 2–20 independent measurements, and were calculated in Prism by use of a logistic fit. E_{max}, % is given in parentheses (NA, not active).

increased conformational rigidity (Table 2). The cyclopentyl amine derivatives, (±)-**7** and (±)-**8**, displayed decreased potency and efficacy. However, the *trans*-cyclopropyl amine (±)-**9**, pyrrolidines **10** and **11**, and piperidine **12a** all showed promising functional activity and selectivity. Of these, **12a** afforded the best combination of potency, selectivity, and low intrinsic clearance in vitro.

In light of the in vitro profile of lead compound **12a**, we set out to explore the structure–activity relationships around this novel *N*-arylpiperidine oxadiazole scaffold. Molecular modeling revealed that **1** and **12a** adopt similar low energy conformations (Fig. 1),[10] suggesting that these two series of molecules share similar binding modes, and may therefore exhibit parallel SAR.[4]

Table 2
Functional GTP-Eu binding assay results for compounds (±)-**7**–**12a** (EC_{50}, μM; E_{max}, %) and $CL_{int.}$ in rat and human liver microsomes (RLM, HLM)[a]

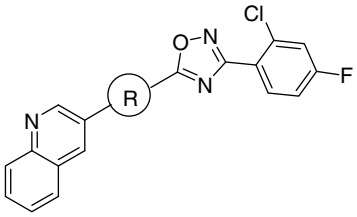

Compound	R	CB_2 EC_{50} (E_{max})	CB_1 EC_{50} (E_{max})	$CL_{int.}$ (μL/min/mg)	
				RLM	HLM
(±)-**7**	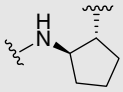	0.465 (73)	2.23 (39)	–	–
(±)-(**8**	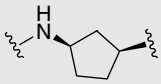	1.60 (77)	NA (4)	–	–
(±)-(**9**	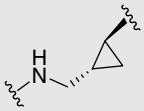	0.099 (110)	NA (8)	193	69
10	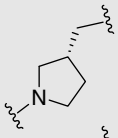	0.086 (116)	1.27 (46)	426	215
11	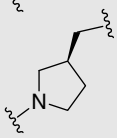	0.140 (109)	1.69 (24)	579	215
12a	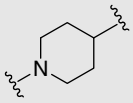	0.089 (101)	3.03 (36)	80	92

[a] The results are expressed as the means SEM for n = 2–20 independent measurements, and were calculated in Prism by use of a logistic fit. E_{max}, % is given in parentheses (NA, not active).

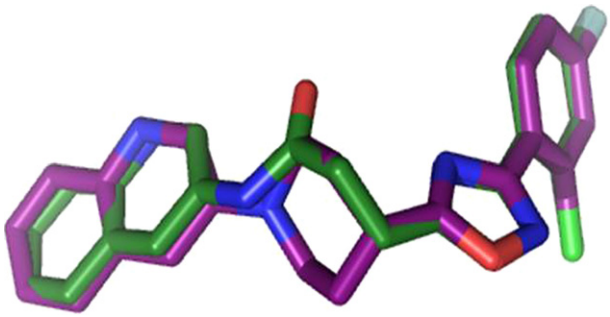

Figure 1. Overlay of amide oxadiazole **1** (green) and piperidine oxadiazole **12a** (purple).

Taking advantage of a modular and divergent synthetic strategy, we held the oxadiazole-aryl substituent (R^2) constant as 2-chloro-4-fluoro-phenyl, and varied the *N*-aryl substituent (R^1, Table 3). Concurrently, fixing the *N*-aryl substituent (R^1) constant as 3-quinoline, we varied the oxadiazole substituent (R^2, Table 4).[11] Our initial survey of R groups was based on the SAR observed in the *N*-aryl amide oxadiazole series and the overlay of low energy conformations for the two scaffolds.

Despite having steric bulk which was comparable to the lead **12a**, compounds such as **12b** with 3,4-di-substituted aryl substituents at R^1 were significantly less potent (Table 3). Upon confirming that the 3-quinoline isomer was clearly preferred to the 4-quinoline isomer **12c**, we quickly discovered that close structural analogs of 3-quinoline afforded the best combination of potency and selectivity (i.e., **12e–i**).

The SAR around R^2 revealed that the 2-Cl substituent was critical for potency (**13a** vs. **13b**, **13c** vs. **13d**, Table 4). Although **13b** was 4-fold more potent than **12a**, it was significantly less selective and less stable in vitro. Although **13d** was equi-potent to **12a** and metabolically stable, it was significantly less selective. The cyclohexyl analog **13f** had a favorable combination of potency, efficacy, and selectivity, but was still a sub-micromolar full agonist of CB_1 with inferior selectivity (23-fold vs. 34-fold) and metabolic stability to that of **12a**. From this initial SAR evaluation, compound **12h** had the best overall potency, efficacy, selectivity, and metabolic stability profile.

On the basis of potency, selectivity, and in vitro stability, selected compounds were further studied in a human cell-based cAMP assay. This assay monitors a distal signaling event from the CB_2 and CB_1 receptors. Activation of CB_2 and CB_1 receptors results in inhibition of adenylate cyclase. Compounds were assessed for

Table 3
Functional GTP-Eu binding assay results for compounds **12b–i** (EC_{50}, μM; E_{max}, %) and $CL_{int.}$ in rat and human liver microsomes (RLM, HLM)[a]

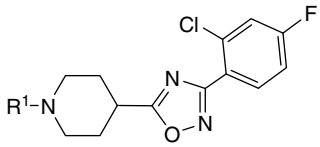

Compound	R^1	CB_2 EC_{50} (E_{max})	CB_1 EC_{50} (E_{max})	$CL_{int.}$ (μL/min/mg)	
				RLM	HLM
12b	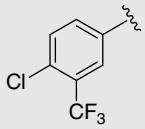	0.376 (93)	NA (2)	–	–
12c	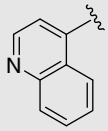	2.86 (35)	NA (2)	–	–
12d	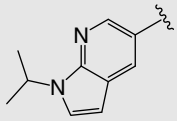	0.340 (88)	NA (13)	–	–
12e	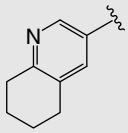	0.019 (113)	0.910 (60)	130	95
12f	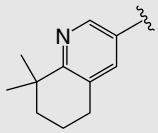	0.032 (108)	0.722 (93)	>399	380
12g	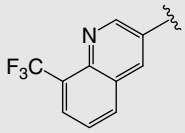	0.016 (106)	0.015 (34)	54	23
12h	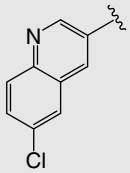	0.007 (120)	1.43 (55)	32	38
12i	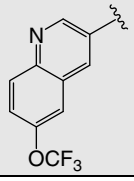	0.003 (110)	0.419 (33)	18	28

[a] The results are expressed as the means SEM for n = 2–20 independent measurements and were calculated in Prism by use of a logistic fit. E_{max}, % is given in parentheses (NA = not active).

their ability to inhibit a forskolin-induced increase in intracellular cAMP (Table 5).[12] Compounds **12a** and **12h** proved superior to (±)-**9** and **10** and comparable to **1** and **6** in potency, efficacy, and selectivity.[13]

The pharmacokinetic parameters of **12h** were assessed in rats following both i.v. and oral administration (Table 6). Compound **12h** was metabolically stable in liver microsomes and displayed low clearance and a long half-life. Following oral administration, reasonable exposure was achieved despite a low oral bioavailability of 2%. **12h** has good permeability and is not a substrate for PgP.[14] We speculate that the low bioavailability is due to poor oral absorption resulting from poor solubility (0.01 N HCl < 1 μg/mL; PBS < 1 μg/mL; SIF 2 μg/mL).[15]

Table 4
Functional GTP-Eu binding assay results for compounds **13a–g** (EC_{50}, μM; E_{max}, %) and $CL_{int.}$ in rat and human liver microsomes (RLM, HLM)[a]

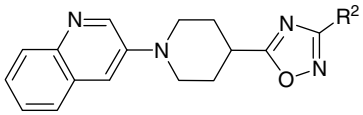

Compound	R^2	CB_2 EC_{50} (E_{max})	CB_1 EC_{50} (E_{max})	$CL_{int.}$ (μL/min/mg)	
				RLM	HLM
13a	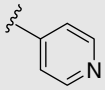	0.313 (53)	NA (8)	–	–
13b	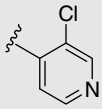	0.024 (103)	0.096 (23)	187	251
13c	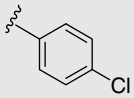	1.78 (26)	2.62 (26)	–	–
13d	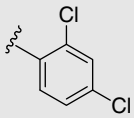	0.080 (99)	0.951 (27)	43	58
13e	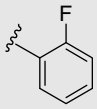	1.55 (89)	NA (8)	–	–
13f		0.026 (113)	0.600 (105)	185	283
13g		1.44 (38)	NA (8)	–	–

[a] The results are expressed as the means SEM for $n = 2–20$ independent measurements, and were calculated in Prism by use of a logistic fit. E_{max}, % is given in parentheses (NA, not active).

Table 5
Cellular cAMP assay results for selected compounds (EC_{50}, μM; E_{max}, %)[a]

Compound	hCB_2 EC_{50} (E_{max})	hCB_1 EC_{50} (E_{max})
1	0.005 (98)	0.559 (49)
6	0.050 (93)	>2 (46)
(±)-**9**	>2 (0)	>2 (1)
10	>2 (23)	>2 (3)
12a	0.017 (95)	>1 (17)
12h	0.011 (102)	>2 (19)

[a] The results are expressed as the means SEM for $n = 2–20$ independent measurements and were calculated in Prism by use of a logistic fit. E_{max}, % is given in parentheses.

Table 6
Pharmacokinetic properties of **12h** in male Sprague–Dawley rats[a]

iv[b]		po[c]	
CL	0.039 L/h/kg	%F	2
Vss	0.365 L/kg	C_{max}	682 ng/mL
$t_{1/2}$	8.9 h	AUC_{0-24h}	5240 ng*h/mL

[a] $n = 3$ animals per study.
[b] Dosed intravenously at 0.5 mg/kg in DMSO.
[c] Dosed orally at 10 mg/kg as a suspension in 2% HPMC/1% Tween80/97% water.

The synthetic routes to **1–11** are detailed in Schemes 2 and 3. Condensation of nitrile **14** and hydroxylamine afforded *N*-hydroxybenzamidine **15**, which was condensed with succinic anhydride to afford the carboxylic acid **2** (Scheme 2). As previously described,[4] *N*-arylamide oxadiazoles such as **1** were prepared by the reaction of intermediate **2** with anilines such as 3-aminoquinoline. Alternatively, carboxylate **1** was converted to the aldehyde **16**, which was then reacted with anilines, under reductive amination conditions, to afford propylamines such as **4**.[4] For the synthesis of mono-methyl propylamine (±)-**5**, 4-oxopentanoic acid **17** was condensed with *N*-hydroxybenzamidine **15** to afford ketone **18**, which underwent a reductive amination with 3-aminoquinoline to provide (±)-**5**. The gem dimethyl propylamine **6** was synthesized beginning with a condensation of *N*-hydroxybenzamidine **15** with anhydride **19** to afford the carboxylic acid **20**, which was converted to the tertiary amine **21** under Curtius conditions. Amine **21** was then coupled with 3-bromoquinoline using a Buchwald-Hartwig amination to afford **6**.[16]

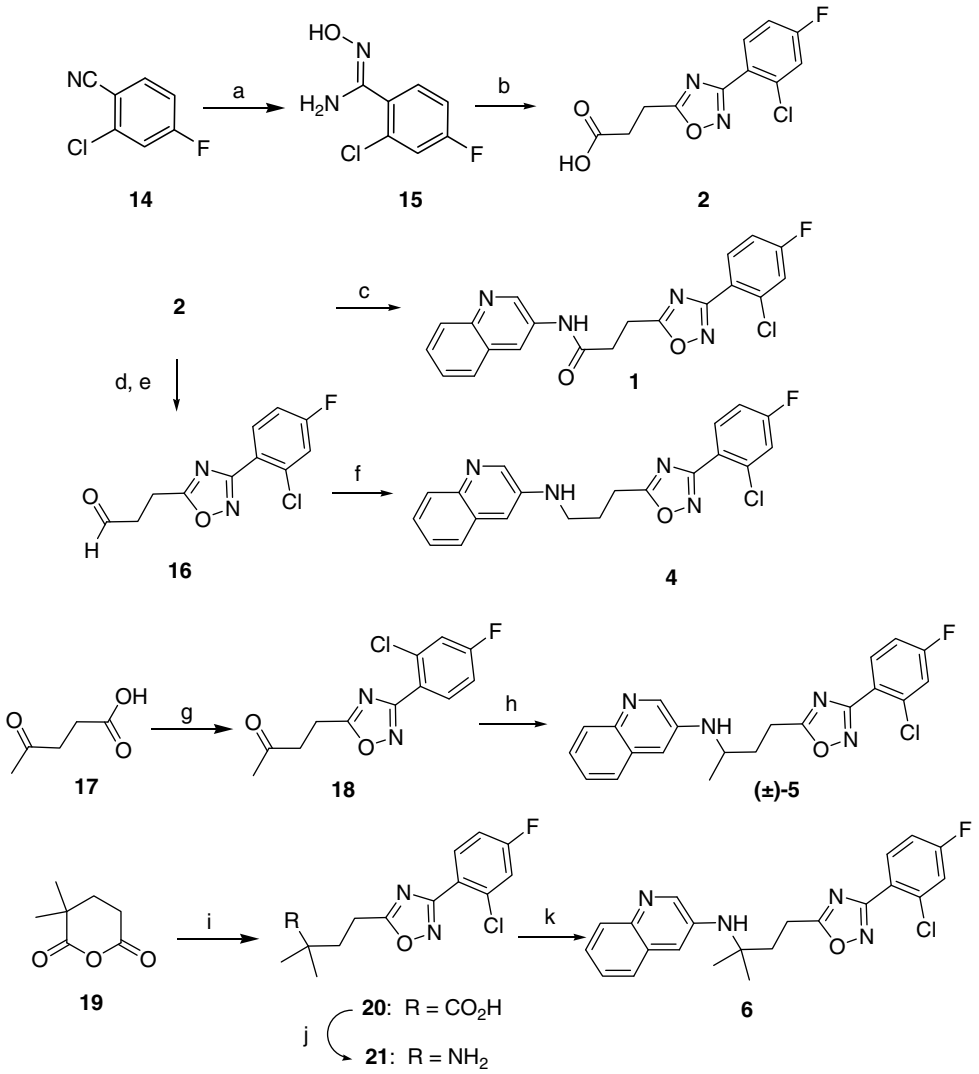

Scheme 2. Reagents and conditions: (a) Hydroxylamine hydrochloride, Na_2CO_3, MeOH/Water (4:1), 95%; (b) Succinic anhydride, DMF, 120 °C, 98%; (c) PS-Carbodiimide, HOBt, 3-aminoquinoline, CH_2Cl_2, 13%; (d) i—TMS-diazomethane, ii—DIBAL-H, CH_2Cl_2/MeOH, 66%; (e) Dess-Martin periodinane, CH_2Cl_2, 84%; (f) 3-aminoquinoline, $NaBH_4$, DCE, 40%; (g) **15**, HOBt hydrate, DIPEA, DMF, 110 °C, 77% (h) 3-aminoquinoline, $NaBH(OAc)_3$, DCE, 3%; (i) **15**, DMF, 120 °C, 90%; (j) DPPA, NEt_3, benzene, 47%; (k) 3-bromoquinoline, Pd_2dba_3, NaO*t*-Bu, X-Phos, toluene, 60 °C, 3%.

The syntheses of (±)-**7**, (±)-**8**, and (±)-**9** were accomplished using oxadiazole formation and reductive amination sequences similar to that applied in the synthesis of (±)-**5** (Scheme 3). Pyrrolidines **10** and **11** were isolated by chiral resolution of the racemate (±)-**32**, which was prepared from amine (±)-**31** using Pd-Xantphos-catalyzed Buchwald-Hartwig amination.[16]

Our synthetic approach to piperidine oxadiazoles allowed for final stage modifications of either of the two aryl termini (Scheme 4). TBTU/HOBt-promoted reaction of 1-Boc-piperidine-4-carboxylate (**33**) with *N*-hydroxybenzamidine **15**, followed by removal of the Boc protecting group, afforded the penultimate piperidine oxadiazole **34**. Finally, *N*-aryl groups (R^1) were installed to afford **12a–i** using a Pd-Xantphos-catalyzed Buchwald-Hartwig amination.[16] These amination conditions were similarly used to afford nitrile **36** from piperidine-4-carbonitrile (**35**) and 3-bromoquinoline. After hydrolysis of the nitrile, the resulting acid **37** was condensed with a variety of *N*-hydroxybenzamidines under the usual conditions to afford **13a–g**.[11]

In summary, structural modifications to the central portion of the *N*-arylamide oxadiazole scaffold were investigated in an effort to improve potency and metabolic stability through increased conformational constraint. These efforts led to the identification of *N*-arylpiperidine oxadiazole **12a** as a novel, potent, selective, full agonist of CB_2. The modular scaffold allowed for the use of expeditious and divergent synthetic routes which provided two-directional SAR in tandem. Our initial lead-optimization efforts have identified **12h** as a highly potent, >200-fold selective, full agonist with promising pharmacokinetics in rodents. We believe that *N*-arylpiperidine oxadiazoles with appropriate PKDM properties could be developed as analgesic agents for the treatment of inflammatory and neuropathic pain.

Acknowledgement

The authors are grateful to Yuan Cheng, and Jim Brown for helpful discussions.

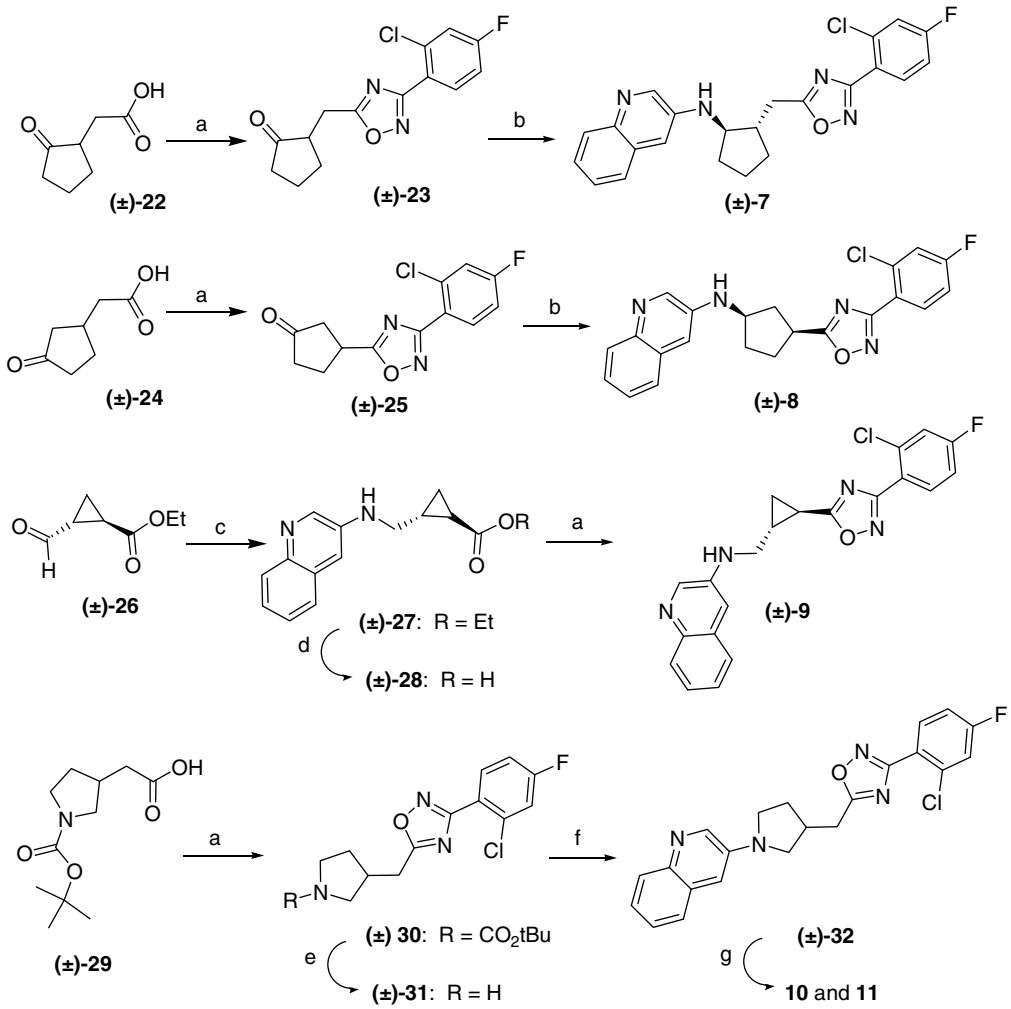

Scheme 3. Reagents and conditions: (a) **15**, HOBt hydrate, DIPEA, DMF, 110 °C, 88% (±)-**23**, 65% (±)-**25**, 15% (±)-**9**, 49% (±)-**3**; (b) 3-aminoquinoline, $NaBH(OAc)_3$, DCE, 5% (±)-**7**, 15% (±)-**8**; (c) 3-aminoquinoline, $NaBH_4$, $Ti(Oi\text{-}Pr)_4$, CH_2Cl_2, 100%; (d) LiOH, THF/MeOH, 75%; (e) TFA, CH_2Cl_2, 98%; (f) 3-bromoquinoline, Pd_2dba_3, NaO*t*-Bu, XantPhos, toluene, 100 °C, 60%; (g) chiral HPLC.

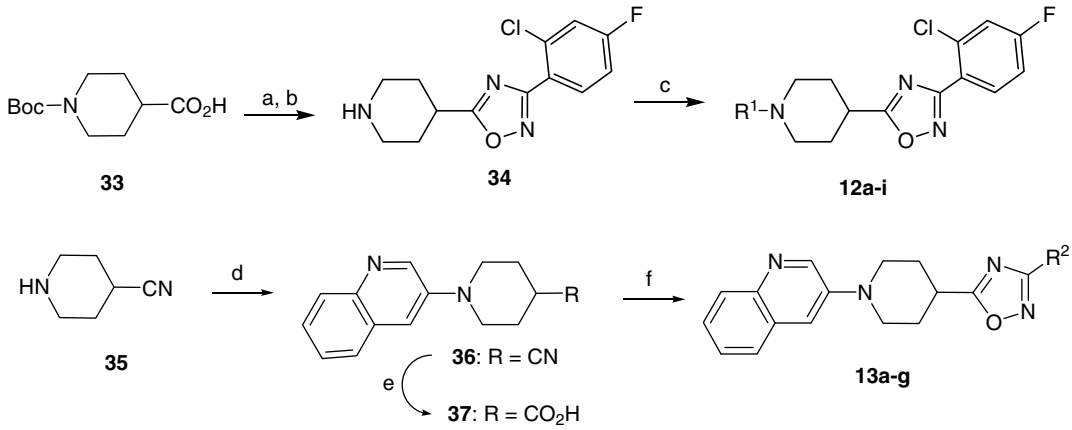

Scheme 4. Reagents and conditions: (a) **15**, TBTU, HOBt, DIPEA, DMF, 100 °C, 55%; (b) TFA, 100%; (c) R^1Br, $Pd_2(dba)_3$, Xantphos, NaO*t*-Bu, toluene, 100 °C, 13–57%; (d) 3-bromoquinoline, $Pd_2(dba)_3$, Xantphos, NaO*t*-Bu, toluene, 100 °C, 90%; (e) H_2SO_4, H_2O, 45%; (f) R^2-*N*-hydroxybenzamidine, TBTU, HOBt, DIPEA, DMF, 100 °C, 21–34%.

References and notes

1. (a) Muccioli, G. *Chem. Biodiv.* **2007**, *4*, 1805; (b) Mackie, K. *Annu. Rev. Pharmacol. Toxicol.* **2006**, *46*, 101; (c) Demuth, D. G.; Molleman, A. *Life Sci.* **2006**, *78*, 549; (d) Lambert, D. M.; Fowler, C. J. *J. Med. Chem.* **2005**, *48*, 1.
2. (a) Campbell, F. A.; Tramer, M. R.; Carroll, D.; Reynolds, J. M.; Moore, R. A.; McQuay, H. J. *BMJ* **2001**, *323*, 13; (b) Abood, M. E.; Martin, B. R. *Trends Pharmacol. Sci.* **1992**, *13*, 201; (c) Johnson, M. R.; Melvin, L. S.; Althuis, T. H.; Bindra, J. S.; Harbert, C. A.; Milne, G. M.; Weissman, A. *J. Clin. Pharmacol.* **1981**, *21*, 271S.

3. (a) Högenauer, E. K. *Expert Opin. Ther. Patents* **2007**, *17*, 1457; (b) Cheng, Y.; Hitchcock, S. A. *Expert Opin. Investig. Drugs* **2007**, *16*, 951; (c) Worm, K.; Zhou, Q. J.; Saeui, C. T.; Green, R. C.; Cassel, J. A.; Stabley, G. J.; DeHaven, R. N.; Conway-James, N.; LaBuda, C. J.; Koblish, M.; Little, P. J.; Dolle, R. E. *Bioorg. Med. Chem. Lett.* **2008**, *18*, 2830; (d) Whiteside, G. T.; Lee, G. P.; Valenzano, K. J. *Curr. Med. Chem.* **2007**, *14*, 917; (e) Ohta, H.; Ishizaka, T.; Tatsuzuki, M.; Yoshinaga, M.; Iida, I.; Yamaguchi, T.; Tomishima, Y.; Futaki, N.; Toda, Y.; Saito, S. *Bioorg. Med. Chem.* **2007**, *15*, 6299; (f) Giblin, G. M. P.; O'Shaughnessy, C. T.; Naylor, A.; Mitchell, W. L.; Eatherton, A. J.; Slingsby, B. P.; Rawlings, D. A.; Goldsmith, P.; Brown, A. J.; Haslam, C. P.; Clayton, N. M.; Wilson, A. W.; Chessell, I. P.; Wittington, A. R.; Green, R. *J. Med. Chem.* **2007**, *50*, 2597; (g) Manera, C.; Cascia, M. G.; Benetti, V.; Allara, M.; Tuccinardi, T.; Martinelli, A.; Saccomanni, G.; Vivoli, E.; Ghelardini, C.; Di Marzo, V.; Ferrarini, P. L. *Bioorg. Med. Chem. Lett.* **2007**, *17*, 6505; (h) Raitio, K. H.; Salo, O. M. H.; Nevalainen, T.; Poso, A.; Järvinen, T. *Curr. Med. Chem.* **2005**, *12*, 1217; (i) Malan, T. P., Jr.; Ibrahim, M. M.; Deng, H.; Liu, Q.; Mata, H. P.; Vanderah, T.; Porecca, F.; Makriyannis, A. *Pain* **2001**, *93*, 239.
4. Cheng, Y.; Albrecht, B. K.; Brown, J.; Buchanan, J. L.; Buckner, W. H.; DiMauro, E. F.; Emkey, R.; Fremeau, R. T. Jr.; Harmange, J. -C.; Hoffman, B. J.; Huang, L.; Huang, M.; Lee, J. H.; Lin, F. -F.; Martin, M. W.; Nguyen, H. Q.; Patel, V. F.; Tomlinson, S. A.; White, R. D.; Xia, X.; Hitchcock, S. A. *J. Med. Chem.* **in press.**.
5. Johnson, M. R.; Melvin, L. S. Full agonist activity was defined as E_{max} equal to 100% efficacy of CP 55,940, a known agonist of both CB_1 and CB_2 receptor. In *Cannabinoids as Therapeutic Agents*; Mechoulam, R., Ed.; CRC Press: Boca Raton, FL, 1986; p 121.
6. The GTP-Eu binding assay is a proximal assay that measures activation of G-protein coupled receptors by the ability of the associated $G\alpha$-protein to bind GTP. Two membrane preparations (B_{max}: 1.7 pmol/mL for both) from Sf9 insect cells co-transfected with human CB_1 or CB_2 and Gai3 were assessed by monitoring binding of a non-hydrolysable GTP analog, GTP-Europium. 3 μM CP55940, a full agonist at both CB_1 and CB_2 receptors, defined 100% efficacy. The procedure was modified from a commercial kit (Perkin Elmer, AD-0167), in that 25 μL of buffer A (50 mM Hepes, 0.1% BSA) containing a certain concentration (0.01 nM to 10 μM) of tested compound was added to 125 μL of buffer B (50 mM Hepes, 0.1% BSA, 10 mM MgCl2, 150 mM NaCl, 5 uM GDP, 10 nM GTP-Europium, 0.0005% Saponin and CB_1 (4.5 μg/well) or CB_2 (14 μg/well) membranes) in a 96-well filtration assay plate that came with the kit. The final DMSO concentration was 1%. The plate was incubated at rt for 45 min followed by filtering and washing twice with 300 μL of cold GTP wash buffer (supplied with the kit) on a vacuum manifold device (Millipore, MAVM 096 0R). The plate was then read in a fluorescent plate reader (Perkin-Elmer Envision) at 615 nm and data were analyzed with Activity Base.
7. Following i.v. dosing of 0.5 mg/kg to male Sprague–Dawley rats, >50% of the dose was converted to **2** for several *N*-arylamide oxadiazoles and *N*-arylpropylamine oxadiazoles. High levels of **2** were consistently observed in plasma samples taken from pharmacodynamic studies of *N*-arylamide oxadiazoles and *N*-arylpropylamine oxadiazoles in rodents.
8. Compounds were considered "not active" if their E_{max} was less than 15% at 10 μM concentration. In these cases an EC_{50} value was not calculated.
9. For other examples, see: (a) Omura, H.; Kawai, M.; Shima, A.; Iwata, Y.; Ito, F.; Masuda, T.; Ohta, A.; Makita, N.; Omoto, K.; Sugimoto, H.; Kikuchi, A.; Iwata, H.; Ando, K. *Bioorg. Med. Chem. Lett.* **2008**, *18*, 3310; (b) Verbist, B. M. P.; De Cleyn, M. A. J.; Surkyn, M.; Fraiponts, E.; Aerssens, J.; Nijsen, M. J. M. A.; Gijsen, H. J. M. *Bioorg. Med. Chem. Lett.* **2008**, *18*, 2574; (c) Ermann, M.; Riether, D.; Walker, E. R.; Mushi, I. F.; Jenkins, J. E.; Noya-Marino, B.; Brewer, M. L.; Taylor, M. G.; Amouzegh, P.; East, S. P.; Dymock, B. W.; Gemkow, M. J.; Kahrs, A. F.; Ebneth, A.; Löbbe, S.; Thome, D.; O'Shea, K.; Dinallo, R.; Raymond, E.; Shih, D-T.; Thomson, D. *Bioorg. Med. Chem. Lett.* **2008**, *18*, 1725; (d) Stern, E.; Muccioli, G. G.; Millet, R.; Goossens, J-F.; Farce, A.; Chavatte, P.; Poupaert, J. H.; Lambert, D. M.; Depreux, P.; Hénichart, J-P. *J. Med. Chem.* **2006**, *49*, 70; (e) Raitio, K. H.; Savinainen, J. R.; Vespäläinen, J.; Latinen, J. T.; Poso, A.; Järvinen, T.; Nevalainen, T. *J. Med. Chem.* **2006**, *49*, 2022; (f) Manera, C.; Benetti, V.; Castelli, M. P.; Cavallini, T.; Lazzarotto, S.; Pibiri, F.; Saccomanni, G.; Tuccinardi, T.; Vannacci, A.; Martinelli, A.; Ferrarini, P. L. *J. Med. Chem.* **2006**, *49*, 5947; (g) Murineddu, G.; Lazzari, P.; Ruiu, S.; Sanna, A.; Loriga, G.; Manca, I.; Falzoi, M.; Dessi, C.; Curzo, M. M.; Chelucci, G.; Pani, L.; Pinna, G. A. *J. Med. Chem.* **2006**, *49*, 7502; (h) Pagé, D.; Yang, H.; Brown, W.; Walpole, C.; Fleurent, M.; Fyfe, M.; Gaudreault, F.; St-Onge, S. *Bioorg. Med. Chem. Lett.* **2007**, *17*, 6183; (i) Lavey, B. J.; Kozlowski, J. A.; Shankar, B. B.; Spitler, J. M.; Zhou, G.; Yang, D-Y.; Shu, Y.; Wong, M. K. C.; Wong, S-C.; Shih, N-Y.; Wu, J.; McCombie, S. W.; Rizvi, R.; Wolin, R. L.; Lunn, C. A. *Bioorg. Med. Chem. Lett.* **2007**, *15*, 783.
10. Low energy confirmations and overlay were calculated using FLAME: Cho, S. J.; Sun, Y. *J. Chem. Inf. Model.* **2006**, *46*, 298–306. MMFF94 energies of conformations are within 1 kcal/mol of lowest energy conformations.
11. All products gave satisfactory analytical data as indicated by 1H NMR and LCMS. Data for **12h** are as follows: ^{1}H NMR (400 MHz, DMSO-d_6) δ ppm 8.94 (d, *J* = 2.8 Hz, 1H), 8.01 (dd, *J* = 8.7, 6.0 Hz, 1H), 7.98 (s, 1H), 7.87 (s, 1H), 7,73 (dd, *J* = 8.8, 2.5 Hz, 1H), 7.59 (d, *J* = 2.5 Hz, 1H), 7.48–7.42 (2H), 3.96 (m, 2H), 3.48 (m, 1H), 3.13 (m, 2H), 2.27 (m, 2H), 2.01 (m, 2H); LCMS EI exact mass calculated for $C_{22}H_{17}Cl_2FN_4O$ 443.05005 *m*/*z* found ($M+H^+$) 443.08362.
12. For cAMP modulation as a read-out of cannabinoid activity see (a) Kaminski, N. E. *Toxicol. Lett.* **1998**, *102–103*, 59; (b) Herring, A. C.; Koh, W. S.; Kaminski, N. E. *Biochem. Pharmacol.* **1998**, *55*, 1013; (c) Howlett, A. C.; Breivogel, C. S.; Childers, S. R.; Deadwyler, S. A.; Hampson, R. E.; Porrino, L. J. *Neuropharmacology* **2004**, *47*, 345. For a complete description of cAMP assay conditions see Ref. Ref. 4.
13. In a hERG binding assay using radiolabeled dofetilite, 12 h had an IC_{50} = 0.5 μM. 12 h was highly selective (IC_{50} and EC_{50} >50 μM) over several other GPCRs (sst4, α1-adreno, β1-adreno, D2, 5HT1A, 5HT2B, CXR2, CCR2b, NK1, μ-opiod, H1, M1).
14. Transport of **12h** across LLC-PK1 cells at 5 μM in the presence of 0.1% BSA. Wild-type: Papp (avg) = 9.95×10^{-6} cm/s; Efflux ratio = 0.9. h-MDR1: Papp (avg) = 10.65×10^{-6} cm/s; Efflux ratio = 0.9.
15. Tan, H.; Semin, D.; Wacker, M.; Cheetham, J. *JALA* **2005**, *10*, 364.
16. Klingensmith, L. M.; Strieter, E. R.; Barder, T. E.; Buchwald, S. L. *Organometallics* **2006**, *25*, 82.